Quantum Electronics **46** (6) 558–566 (2016)

HOLOGRAPHIC SENSORS DOI: 10.1070/QEL14915

Determination of the parameters of a holographic layer from its spectral characteristics

A.A. Kraiskii, A.V. Kraiskii

Abstract. **Methods for estimating the main parameters of holographic sensors (refractive index modulation depth and hologram thickness) from transmission spectra in the absence of absorption and light scattering are discussed. The consideration is performed for layers oriented parallel to the holographic layer surface under normal light incidence. Direct numerical solution of the problem of light propagation in a periodic nonabsorbing medium is used to study the reflection and transmission spectra of the holographic layer in a wide range of variation in its thickness and the refractive index modulation depth. A classification of the reflection regimes from the holographic layer is proposed (from weak reflection to the photonic crystal regime). A comparison with the results obtained by the coupled-wave analysis is performed, and the limitations of this method at a significant spectral detuning from resonance and under conditions of strong reflection are revealed. It is shown that the main hologram parameters can be estimated from the experimental transmission spectrum of the phase hologram (in the case of strong reflection) based on the spectral dip parameters.**

Keywords: *holographic sensors, light propagation, periodic medium, determination of hologram parameters, coupled waves.*

1. Holographic sensors [1, 2] form a new class of diagnostic devices. Such a sensor is based on a Denisyuk hologram (a layered periodic structure with periodically changing optical properties). For definiteness, we will refer to the period of this structure as the interference-layer thickness. Under the conditions considered below, it is approximately half the wavelength in the medium. The thickness of the entire periodic structure will be referred to as the holographic layer thickness or the hologram thickness. Under certain conditions [2], the medium forming the holographic layer undergoes nonuniform compressions or extensions, and the medium becomes aperiodic, i.e., smooth spatial variations in the interference-layer thickness and/or refractive index occur in it.

This hologram has a narrow reflection spectrum. The interaction of a tested material with the materials intentionally incorporated into the matrix leads to a change in the degree of matrix swelling and, correspondingly, to a change in the reflected light wavelength, which characterises the tested component content. For a purely phase hologram with strictly periodic layers, under conditions of weak reflection, the spectral width of reflected light is inversely proportional to the holographic-layer thickness. In the case of strong reflection, the dependence is more complicated (see below). Obviously, to make sensors operate correctly, one must be able to determine the layer parameters (primarily, the refractive index modulation depth and the layer thickness).

Holographic layers on the basis of silver halides are most popular. We will consider bleached holograms based on nanograins of transparent silver compounds, in which absorption and light scattering losses are negligible. To apply correctly holographic layers of sensors, one must know which layer parameters affect the reflection spectrum and how they do it.

The propagation of waves of different nature in periodic structures has been studied in detail for many years [3, 4], and these studies are being continued now. These processes can be described using computer simulation methods; however, for some reasons, various approximate methods are often applied to solve practical problems. Concerning one-dimensional optical problems, the main principles of constructing solutions for media with sinusoidally changing optical constants were described in [5–8] (an example of the latest studies in this field is [9]). Nevertheless, computer-aided calculations are inevitable when practical problems must be solved.

An additional difficulty is that the structure often becomes aperiodic. The fundamentals of the calculations of multilayer aperiodic structures with a step profile were considered, e.g., in [10]. The matrix method [10, 11] is widely used to calculate these structures (periodic and aperiodic coatings, mirrors) in the optical and X-ray ranges.

In the case of strictly periodic layers with a sinusoidally changing profile, researchers apply the coupled-wave analysis [5–7], with makes it possible to obtain easily transmission and reflection spectra in a wide range of diffraction efficiencies and the field distribution over the layer depth. The simplest approach is to consider the light propagation in media with low reflectance; however, in the general case, the expressions are complicated and require numerical calculations.

Note that the problems of light propagation in Denisyuk holograms have been widely discussed since the beginning of the 1960s; however, researchers were mainly interested in the problems related to the behaviour of reflectance in dependence of the hologram parameters (see, e.g., [8]).

The measured parameter of holographic sensors is the position of the reflection band maximum. Except for this parameter, no other optical properties of holographic sensors had been discussed in the literature until 2010, when our study [2] was published. Two problems were revealed in that work. The first one is the sharp (by almost an order of magnitude)

A.A. Kraiskii, A.V. Kraiskii P.N. Lebedev Physics Institute, Russian Academy of Sciences, Leninsky prosp. 53, 119991 Moscow, Russia; e-mail: kraiski@sci.lebedev.ru

Received 26 June 2012; revision received 25 February 2014
Kvantovaya Elektronika **46** (6) 558–566 (2016)
Translated by Yu.P. Sin'kov

change in the reflectance with a change in the tested-solution acidity, which is accompanied by a significant change in the centre wavelength of reflected radiation and is related to the structural transformation of the layer and the variation in the ion concentration in the solution. The reflectance may change from weak (~0.1) to very strong (~1). The second problem is the variation in the spectral shape of the reflection band: its broadening and, under certain conditions, significant violation of symmetry and occurrence of some substructures in it. In particular, in many transition processes accompanied by significant changes in swelling, which manifest themselves in the spectral shift of the reflection band, one first observes a significant line broadening and occurrence of band structuring, which is then transferred over the spectrum at small variations in its structure [2, 12]. Since changes in the spectral shape are not always related to variations in the total reflection, it is evident that the holographic layer matrix swells nonuniformly over depth.

In the final stationary state, the band narrows to the initial state in many cases; specifically, the ratio of the wavelength in the reflection maximum to the width of the reflection band is recovered (the value of this ratio can be related to the number of effectively reflecting layers). However, this does not occur always, which, most likely, indicates violations of periodicity.

When carrying out measurements, a natural desire is to increase the hologram reflectance. However, in the case of strong reflection, the incident light will rapidly attenuate in the bulk of the hologram, thus reducing the number of effective working layers (below, we refer to the number of the latter as the effective number of layers). The geometric size related to the effective number of layers will be referred to as the effective layer thickness. Thus, strong reflection leads to an increase in the spectral bandwidth of reflected light and, therefore, increases the error in measuring the tested-component content. Therefore, the operational conditions must be chosen so as to exclude the reflectance overshoot above the maximum allowable value in the entire working range.

The broadening caused by the layer aperiodicity may also reduce the measurement accuracy. Note that the study of the kinetics of sensor responses may gain a deeper insight into the processes occurring in the layer. Having successfully solved this problem, one can obtain phenomenological data not only on the amount of a particular material but also on the optical characteristics of the solution in the matrix, which may expand the range of problems solved by applying sensors.

Therefore, the operation regime of the holographic layer should be optimised. It is necessary to perform an adequate calculation of the optical parameters of the system, primarily, the reflection and transmission characteristics, including the shape of the reflected-light band, and determine the degree of attenuation for the light transmitted through the layer. The propagation of waves in a medium with a harmonic spatial dependence of permittivity can be considered in terms of the coupled-wave analysis [5–7], independent of the reflection magnitude. If the spatial dependence of the permittivity contains several harmonics (with a nonsinusoidal permittivity profile), the coupled-wave analysis is also applicable; however, the mathematics is more complicated in this case. Note that, along with a nonuniform distribution of the interference layer thickness over depth, spatial inhomogeneity of the refractive index modulation depth may also occur. As far as we know, the solution for these media in the general form has not been analysed in the literature.

Most of the aforementioned studies were aimed at solving the forward problem, i.e., determining the transmission and reflection spectra of a layer with its parameters specified. The only exception is the studies devoted to multilayer coatings, where a coating design (materials of layers and their thickness, and sequence) is chosen for a specified (rather broadband) spectrum [11, 13, 14]. This problem has its own specificity, because it generally considers a stepwise profile of a single layer, and the simple matrix method can be applied to it. Recently, nonideal step coatings with a transition layer between neighbouring layers have also been investigated [14].

The problem discussed above is fairly universal. It contains a large set of free parameters and some criteria of correspondence, which are comapred with the mismatch functional (depending also on the spectral shape) in the space of fitting parameters. This multiparameter functional may have a complex structure, with a large number of local minima (traps). Generally, the problem of searching for the global minimum is stated; however, in some cases, the number of close-to-global minima may exceed unity.

A peculiar inverse problem must be solved in the case of sensors used for analytical purposes. Here, the case in hand is not the fitting of layer parameters to an arbitrary spectrum but the estimation of the parameters of a periodic depth-limited medium (layer thickness, refractive index modulation depth, and distance between neighbouring layers) from its spectrum. Here, the structure of the mismatch function in the fitting-parameter space may be radically different. In this study, we will restrict ourselves to a very simple fitting problem: consideration of a strictly periodic medium and fitting of the main parameters of the Bragg dip (its position, width, and relative amplitude) by varying the main hologram parameters (relative modulation depth of refractive index and holographic layer thickness). We will also consider the one-dimensional problem, in which periodic layers are parallel to the holographic layer boundaries, and the wave vector of the incident wave is oriented normally to the layers.

The main problems to be solved in this stage of our investigations is to control the sensor operation regime and determine the parameters of the medium under all possible conditions for holographic layer operation, including the layer aperiodicity and inhomogeneous refractive index modulation depth. The main purpose of this study is to estimate the parameters of a nonabsorbing holographic layer (its thickness and refractive index modulation depth) from an experimental spectrum using a computer model of plane-wave propagation in a strictly periodic layer of finite thickness.

2. Let us consider different operation regimes of the holographic layer. It is well known [5–7] that, in the case of a strictly periodic sinusoidal medium, there are three parameters completely determining the field propagation regime and the formation of the reflection spectrum: structure period, layer thickness H, and refractive index modulation depth Δn. Based on the reflection bandwidth, provided that the reflection is weak (the weakness criteria will be considered below), one can easily determine the number of interference layers (i.e., the hologram thickness) in the case of strictly periodic layers. The refractive index modulation depth can be found from the amplitude of the peak in the reflection band (note that the reflectance must be calibrated). However, this problem can be solved in another way.

The transmission spectrum contains a Bragg dip (Fig. 1), the parameters of which (position, depth, and width) are related to the reflection band characteristics. Thus, the prob-

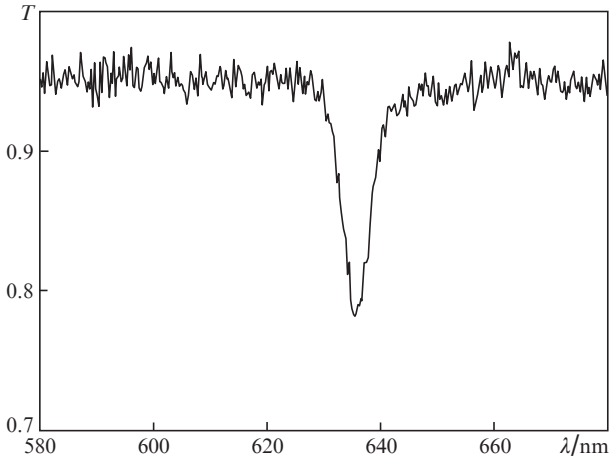

Figure 1. Experimental transmission spectrum for a phase hologram.

lem to be solved can be formulated as follows: the parameters of a hologram must be determined from the characteristics of its transmission spectrum, i.e., the resonant wavelength and the depth and width of the spectral dip.

First we will solve the forward problem: calculate the reflection and transmission spectra of a layer of specified thickness H and refractive index modulation depth Δn and analyse the dependences of spectral parameters A (relative dip depth) and $\Delta\lambda$ (FWHM) on H and Δn, obtained for a set of thicknesses and modulation amplitudes.

Then we can pass to the main problem: estimation of the layer parameters from the spectral characteristics. This will be done by the fitting method: we will solve the forward problem using some H and Δn values and obtain as a result a transmission spectrum with a dip of depth A and width $\Delta\lambda$. Then the H and Δn values will be chosen so as to make parameters A and $\Delta\lambda$ of the calculated and experimental spectra coincide.

3. The light propagation in periodic structures with known parameters was investigated in detail by coupled-wave analysis with allowance for two waves [5–7]. Within this approach, the transmittance and reflectance can be found from a system of analytical expressions. However, this approximation is valid for only the central maximum. Figure 2 shows the results obtained by us based on the approaches described in [5–7] and the results of the direct calculation, which is considered below. On the scale of Fig. 2a, the curves obtained by both methods coincide; however, at a larger magnification, one can observe an asymmetry in the amplitudes of lateral maxima (Fig. 2b), which is more pronounced in the case of coupled-wave analysis [5–7] as compared with direct calculation. The differences in the positions of lateral maxima and minima are also pronounced. An increase in the detuning of the incident radiation wavelength from the Bragg conditions increases the difference in the results obtained by the coupled-wave analysis (according to Kogelnik [5]) and the direct calculation. This difference increases also with an increase in the permittivity modulation depth.

4. Let us consider the case of small refractive index modulation and, therefore, of the weak reflection. We will divide

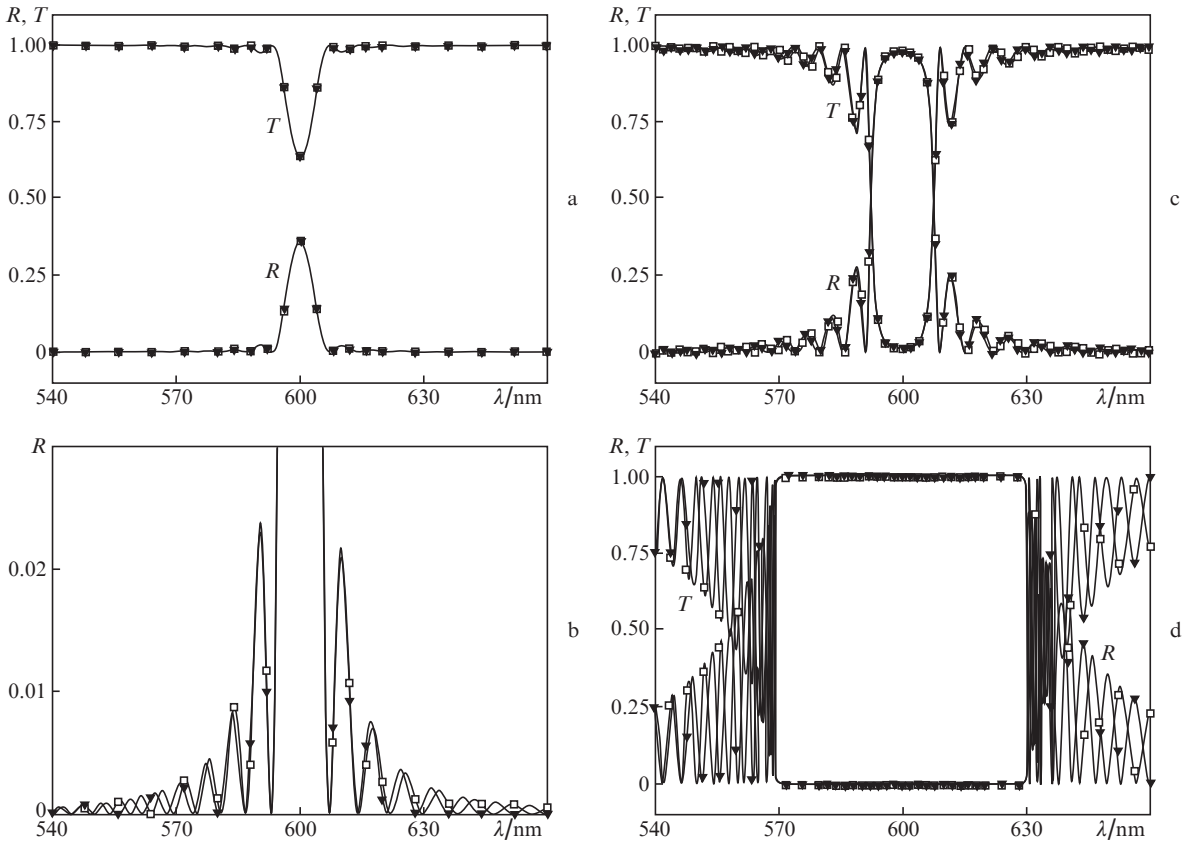

Figure 2. Reflection and transmission spectra obtained by numerical calculation (filled symbols) and calculated in terms of the coupled-wave analysis (open symbols) for (a, b) weak reflection, (c) strong reflection in the regime of photonic crystal formation, and (d) very strong reflection in the photonic crystal regime.

the holographic layer of thickness H into infinitely thin layers of thickness $\mathrm{d}x$ with somewhat differing refractive indices $n(x)$. Let us consider two such layers with refractive indices n and $n + \mathrm{d}n$. The electric field of a wave reflected from the interface between these layers can be written as (see [4])

$$\mathrm{d}E = -\frac{\mathrm{d}n}{2n(x)} E_0(x). \tag{1}$$

We neglect the multiple reflections of light in the layer and the variation in the refractive index in the denominator in view of their smallness; then, the wave reflected by the hologram will be determined by the sum of waves (1) with a corresponding phase delay. The field is described by the expression

$$E = \frac{E_0}{2n_0}\int_0^H \exp(2\mathrm{i}\varphi)\left(-\frac{\mathrm{d}n}{\mathrm{d}x}\right)\mathrm{d}x. \tag{2}$$

The refractive index is given by the formula

$$n(x) = n_0 + \Delta n\cos\left(2\pi\frac{x}{\Lambda} + \varphi_0\right), \tag{3}$$

where n_0 is the average refractive index; x is a coordinate in the direction into layer depth; Λ is the refractive index modulation period; and φ_0 is phase, which determines the position of sinusoid with respect to the holographic layer and is set when photoemulsion is exposed. The field phase in (2) can be written as

$$\varphi = \int n(x)k\,\mathrm{d}x, \tag{4}$$

where k is the wave number of the incident light in vacuum. Since relation

$$\left|\Delta n\frac{\Lambda}{\lambda}\left[\sin\left(2\pi\frac{x}{\Lambda} + \varphi_0\right) - \sin\varphi_0\right]\right| \ll 1 \tag{5}$$

($\lambda/n_0 \sim 2\Lambda$; $\Delta n \ll 1$; λ is the wavelength of incident light in vacuum) holds true, the integral in (4) over the variable part of the refractive index is small and

$$\varphi \approx n_0 kx. \tag{6}$$

A conventional approach is to integrate (2) with allowance for (6), neglecting small first-order values. In sum,

$$E = -E_0\frac{\pi\Delta n}{2\mathrm{i}n_0}\frac{H}{\Lambda}\exp[\mathrm{i}(n_0k - k_0/2) + \mathrm{i}\varphi_0]\frac{\sin[(n_0k - k_0/2)H]}{(n_0k - k_0/2)H}, \tag{7}$$

$$I = I_0\left\{\frac{\pi\Delta n}{2n_0}\frac{H}{\Lambda}\frac{\sin[(n_0k - k_0/2)H]}{(n_0k - k_0/2)H}\right\}^2,$$

where $k_0 = 2\pi/\Lambda$.

The intensity of the maximum is

$$I_{\max} = I_0\left(\pi\frac{\Delta n}{2n_0}\frac{H}{\Lambda}\right)^2. \tag{8}$$

Note that the band FWHM is

$$\Delta\lambda = 0.886\frac{\lambda^2}{2n_0H} = 0.886\frac{\lambda}{N}, \tag{9}$$

where N is the number of interference layers.

Function (7) has a simple form and is convenient for application; it is symmetric with respect to k_0 (the wave vector corresponding to the centre wavelength in the reflection spectrum) in the space of wave numbers, but its accuracy is not very high. However, it is quite applicable in many cases, especially for estimations. The concepts of the effective thickness and number of layers stem from (9), when H_{eff} and N_{eff} (the effective thickness and number of layers, respectively) are purely formally determined with known n_0, λ, and $\Delta\lambda$ values. A more exact expression, with allowance for the small values rejected when deriving (7), has the form

$$E \approx -B\left\{A\frac{2n_0}{2n_0 + \Delta n\cos\varphi_0} + \frac{\mathrm{i}\exp[-\mathrm{i}(n_0k - k_0/2)H - \mathrm{i}\varphi_0]}{(k_0/2)H}\cos\varphi_0\right\}, \tag{10}$$

where

$$B = E_0\frac{\pi\Delta n}{2\mathrm{i}n_0}\frac{H}{\Lambda}\exp[\mathrm{i}(n_0k - k_0/2)H + \mathrm{i}\varphi_0]; \tag{11a}$$

$$A = \left\{\left[\frac{\sin[(n_0k - k_0/2)H]}{(n_0k - k_0/2)H} - \exp[\mathrm{i}(k_0H - 2\varphi_0)]\right.\right. \times\frac{\sin[(n_0k + k_0/2)H]}{(n_0k + k_0/2)H} - \frac{\mathrm{i}\cos\varphi_1}{(k_0/2)H} \left.\left.\times\exp[i(n_0k + k_0/2)H - i\varphi_0]\right]\right\}; \tag{11b}$$

and φ_1 is the phase of the variable part of the refractive index in the output plane. Formula (10) takes into account the first-order values (which are generally rejected): the term with $n_0k + k_0$, which is also related to the reflection from the periodic structure [the second summand in (11b)], takes into account the reflection from the boundaries [the third term in (11b) and the addend in (10) describe the reflection from the output and input planes, respectively]. All these three terms may contribute to the spectral asymmetry. The factor after A in (10) describes the attenuation of the reflected light, emerging from the hologram bulk, in the input plane. In the calculations described below, it was assumed that the average refractive index of the layer coincides with the refractive index of the environment. If the refractive index does not undergo a jump at the boundaries, the third term in (11b) and the addend in the parentheses in (10) become zero, and the asymmetry on the whole is determined by the second term in (11b).

5. To solve the problem in the general case, we will perform direct numerical calculation of the wave propagation problem. We will consider the case of normal incidence of light on a hologram (in practice, the wave is incident at a small angle, which will be neglected). In this approximation, the electric field vector is oriented perpendicular to the wave vector of the periodic structure, and the field satisfies the equation

$$\frac{\mathrm{d}^2u(x)}{\mathrm{d}x^2} - k^2\varepsilon(x)u(x) = 0, \tag{12}$$

where $k = \omega/c$.

In most studies, the permittivity modulation is considered to be harmonic. One can easily perform generalisation to the case of anharmonic modulation. The field in the propagation

region of light incident on the hologram (region 1) is formed by the incident [$E_f = E\exp(ikz)$] and reflected [$E_r = E_1\exp(-ikz)$] waves. In region 3, the field is formed by the transmitted wave $E_{tr} = E_3\exp(ikz)$. The permittivity modulation region (2) is divided into intervals by points M (i.e., a mesh is introduced). The field at point M is taken in the form

$$
\begin{aligned}
&{}_M E_2 = C \ (C = E_3 \text{ is unknown}),\\
&{}_M E_2' = ikC.
\end{aligned}
\tag{13}
$$

These equations were derived from the continuity condition for the field and its derivative. Then, using the fourth-order Runge–Kutta method, we found the field values from Eqn (12) at all $M-1$ grid points (specifically, we determined the ${}_i\tilde{E}_2$ value: the ratio of the field ${}_iE_2$ to the unknown constant C, because, in view of the linearity of (12), the field ${}_iE_2$ at each point of region 2 is proportional to this constant).

Then the fields were matched at the interface between regions 1 and 2:

$$
E + E_1 = {}_1\tilde{E}_2 C, \quad ikE - ikE_1 = {}_1\tilde{E}_2' C. \tag{14}
$$

In these equations, the incident-wave field amplitude E is known, and the amplitude ${}_1\tilde{E}_2$ (${}_1\tilde{E}_2 = {}_1E_2/C$) was determined numerically. Based on Eqns (14), we find the amplitudes of the transmitted [E_3 (= C)] and reflected (E_1) waves. In addition, the formula ${}_iE_2 = {}_i\tilde{E}_2{}^*C$ is used to determine the field in the hologram region.

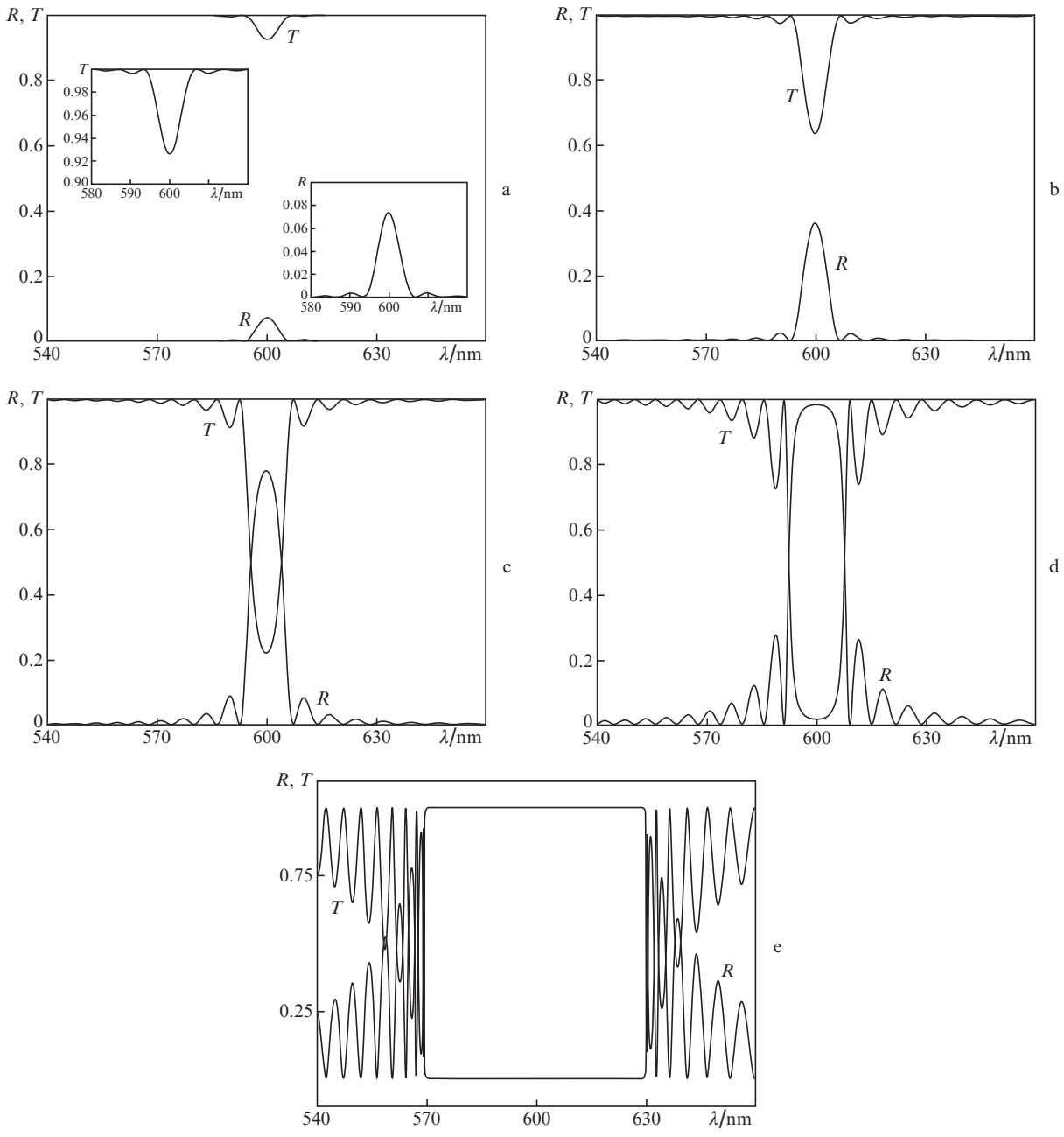

Figure 3. Reflection and transmission spectra for the cases of (a) weak, (b) intermediate, and (c) strong reflection from a hologram, (d) in the regime of photonic crystal formation, and (e) in the photonic crystal regime.

6. Let us now classify the sensor operation regimes as function of the reflection spectrum parameters. In the case of weak reflection (we define it as the regime in which the ratio of the maximum in the reflection spectrum to the incident light intensity is below 0.1), the shape of this spectrum is described by the function $\sin x/x$ (see Fig. 3).

With an increase in the reflectance from 0.1 to 0.4, the spectral shape begins to change: the vertex of the reflection peak becomes slightly flattened, but it can still be approximated by the function $\sin x/x$ with a rather high accuracy. The thickness H_{eff} is close to the holographic-layer thickness H. This regime will be referred to as intermediate reflection.

Strong reflection occurs at reflectances ranging from 0.4 to 0.865. In this regime, the reflection peak vortex is flattened (a dip arises in the spectral dependence of the second derivative), and H_{eff} becomes smaller than the layer thickness, whereas the field penetration depth into the holographic layer becomes comparable with the layer thickness.

With a further increase in the reflectance, the field penetration depth into the layer amounts from 1 to 0.2 of the holographic-layer thickness.

The regimes with smaller penetration depths can be considered as photonic crystal formation regimes. For example, for a sample of thickness $H = 20$ μm, regimes of weak (Fig. 3a), intermediate (Fig. 3b), and strong (Fig. 3c) reflection are implemented at $\Delta n/n_0 = 0.002$, 0.005, and 0.01, respectively; $\Delta n/n_0 = 0.02$ corresponds to the photonic crystal formation regime (Fig. 3d); and, at $\Delta n/n_0 = 0.1$, well-developed band gaps are formed (Fig. 3e), and one can speak about the formation of a photonic crystal.

Figure 4 shows the dependences of the relative dip depth A on the refractive index modulation depth Δn and thickness H of the holographic layer. At small modulation depths and thicknesses, the relative dip depth A behaves, in correspondence with formula (8), as H^2 (Fig. 4a) and $(\Delta n)^2$ (Fig. 4b). Then it tends to a constant value: $A = 1$.

The dependences of the width $\Delta\lambda$ of Bragg transmission minimum on the same parameters are presented in Fig. 5. At small H, these dependences behave as H^{-1} [i.e., according to formula (9)]. With an increase in H, the reflection becomes significant and the effective thickness H_{eff} becomes smaller than the total thickness H. Since $\Delta\lambda \sim H_{\text{eff}}^{-1}$, the dependences deviate from H^{-1} (Fig. 5a). With a change in Δn, the width $\Delta\lambda$ first remains constant and then linearly depends on Δn (Fig. 5b). The reason is that an increase in the modulation amplitude Δn leads to an increase in reflection, and, under strong reflection, the reflected wave is formed at a smaller depth H_{eff}.

Thus, the dependences of the relative dip depth A in the spectrum and the width $\Delta\lambda$ of the Bragg transmission minimum on the hologram parameters are monotonic, due to which one can construct an algorithm of searching for the hologram parameters proceeding from the spectral characteristics; i.e., to solve the inverse problem.

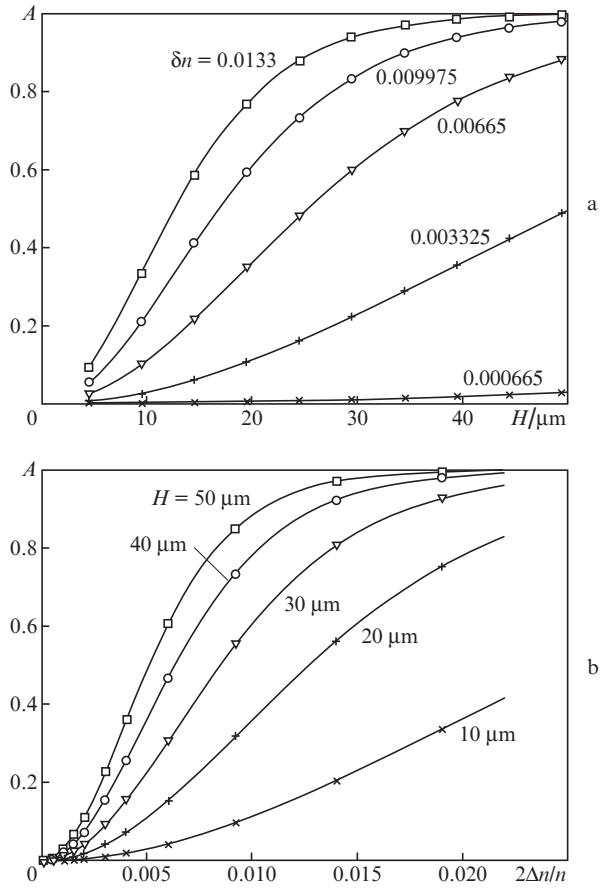

Figure 4. Dependences of the relative dip depth in the transmission spectrum (a) on the thickness of holographic layer at different refractive index modulation depths and (b) on the refractive index modulation depth at different layer thicknesses.

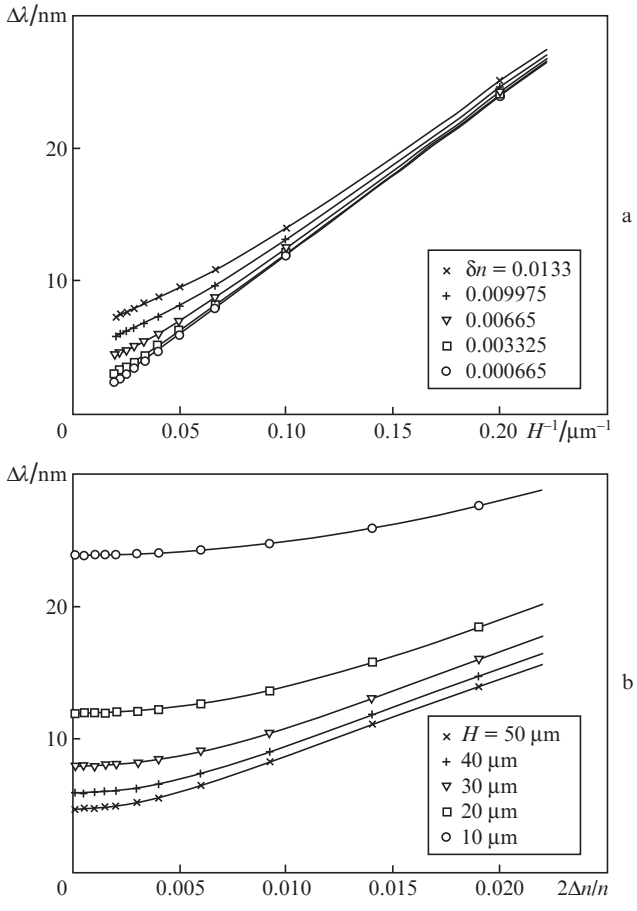

Figure 5. Dependences of the dip width in the transmission spectrum (a) on the inverse thickness of holographic layer at different refractive index modulation depths and (b) on the refractive index modulation depth at different layer thicknesses.

7. Figure 6 shows an experimental spectrum of a bleached hologram. The refractive index of the solution is $n = 1.33$. The dip parameters, determined when fitting by a function equal to the sum of a Gaussian function and a constant background, were found to be $\Delta\lambda_{exp} = 6.16$ nm, $\Delta\lambda_{exp} = 635.85$ nm, and $A_{exp} = 0.16$. First we found the λ_{exp} value and then performed fitting of the two remaining parameters. We used a previously calculated set of dip depths A and widths $\Delta\lambda$ in some range of hologram thicknesses H and refractive index modulation amplitudes Δn. The forward problem of light propagation in a medium was solved for H and Δn, and the transmission spectrum (for which the dip parameters were determined) was calculated. If the mismatch between the dip depth A and width $\Delta\lambda$ and the corresponding experimental values was intolerable, the H and Δn values were varied to minimise the function

$$\Psi = \left(\frac{\Delta\lambda - \Delta\lambda_{exp}}{\Delta\lambda_{exp}}\right)^2 + \left(\frac{\Delta A - \Delta A_{exp}}{\Delta A_{exp}}\right)^2. \qquad (15)$$

The programme performing variation in H and Δn yielded a spectrum with a dip depth A and width $\Delta\lambda$ maximally close to the corresponding parameters of the experimental spectrum. Their values for the spectrum presented in Fig. 6 are $\Delta n = 0.0039$ and $H = 22.8$ μm. Expression (9) yields the effective thickness $H_{eff} = \lambda N_{eff}/(2n) = 21.86$ μm for the same spectrum ($N_{eff} = 0.886\lambda/\Delta\lambda = 91.4$). Thus, the thickness found by fitting the spectrum exceeds the effective thickness by 4.3%.

For a spectrum with a smaller dip depth ($A_{exp} = 0.062$, reflectance less than 10%) and significant dip width in the transmission spectrum ($\Delta\lambda_{exp} = 17.03$ nm), for the Bragg dip minimum located at $\lambda_{exp} = 665.04$ nm, the holographic layer parameters are as follows: $\Delta n = 0.0077$, $H = 8.97$ μm, $N_{eff} = 0.886\lambda/\Delta\lambda = 34.6$, and $H_{eff} = \lambda N_{eff}/(2n) = 8.65$ μm. This set is consistent with the fact that the thickness found from the spectrum slightly exceeds (by 3.5%) the effective thickness.

8. A noteworthy feature of all experimental spectra reported above is the absence of lateral maxima, which are characteristic of reflection spectra from periodic structures. At the same time, Fig. 6 demonstrates a weak 'excrescence' near the boundary of the central maximum (on the right from it), which corresponds to the first lateral maximum. It is especially pronounced in Fig. 7, which shows the transmission spectrum of a hologram based on silver emulsion, in which light absorption and scattering by silver nanograins occurred. The dip was observed against a wide Rayleigh background, decaying to zero at short wavelengths. After subtracting the background and adding a constant background corresponding to the long-wavelength transmission, the dip was approximated by a Gaussian function. The spectrum parameters were found to be $\Delta\lambda_{exp} = 10.2$ nm, $\lambda_{exp} = 620.7$ nm, and $A_{exp} = 0.49$. The fitting procedure yielded $\Delta n = 0.011$ and $H = 15.9$ μm, and an estimate according to formula (9) at $N_{eff} = 0.886\lambda/(\Delta\lambda) = 54.0$ gave $H_{eff} = \lambda N_{eff}/(2n) = 12.6$ μm. In this case, the reflection is strong (from 40% to 86.5%), and the found effective thickness is smaller by 20%. However, in this case, one must take into account that the transmitted wave is attenuated not only due to the energy transfer from the transmitted wave to the reflected wave but also as a result of light scattering and absorption by silver particles. In sum, the background in the wavelength range of the minimum of the Bragg transmission band is about 50% of its value on the long-wavelength edge. The damping at the resonant wavelength should be approximately the same; this circumstance also reduces the effective number of layers and contributes to the observed broadening of the transmission band. Therefore, the thus obtained parameters in the presence of light absorption and scattering are only estimates. To obtain a more exact solution of this problem, one must take into account the attenuation of light propagating in a medium with allowance for scattering and absorption.

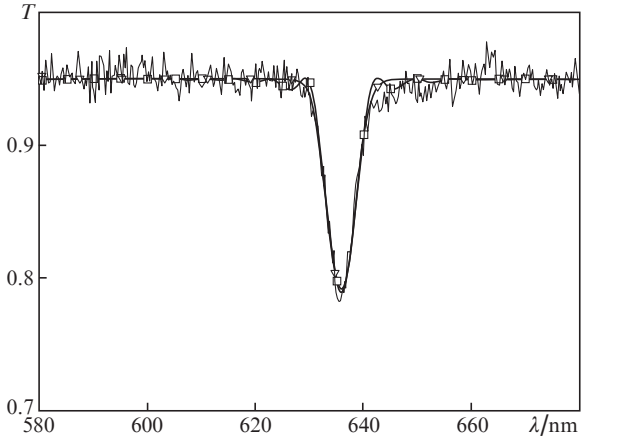

Figure 6. (–) Transmission spectrum of a phase hologram in the case of weak reflection and its approximations (▽) by a Gaussian function and (□) with the aid of direct calculation.

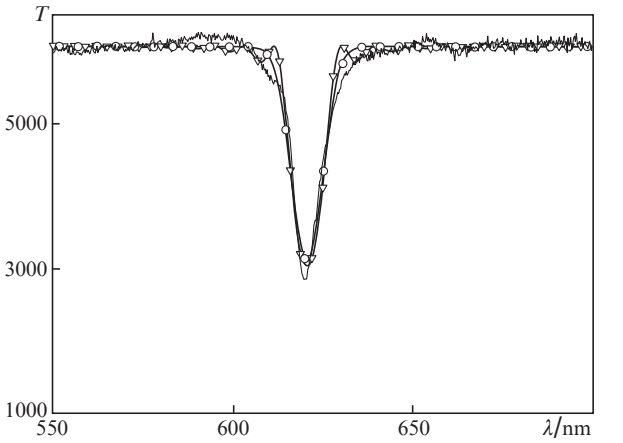

Figure 7. (–) Transmission spectrum of a hologram based on silver emulsion and its approximations (○) by a Gaussian function and (▽) with the aid of direct calculation.

The spectrum in Fig. 7 exhibits pronounced 'excresences' on the right and left from the central maximum. They may be related to the finite width (5.5 nm at half maximum) of the instrumental function of the spectrometer with a fibre input, which is shown in Fig. 8a. Figure 8b presents a calculated spectrum of reflected light for a sinusoidal grating at $H = 20$ μm and $\Delta n = 0.01$ (the spectral width of reflected light is 6.4 nm), the instrumental function, a convolution of these two functions, and their approximation by a Gaussian function with a width of 7.7 nm. In Fig. 8c, the same curves are given on an enlarged scale over the ordinate axis. It can be seen that the central part of the maximum (more than 6% of the maximum value) is approximated well by a Gaussian function; the lateral maxima are smoothed out to a great extent (compare with

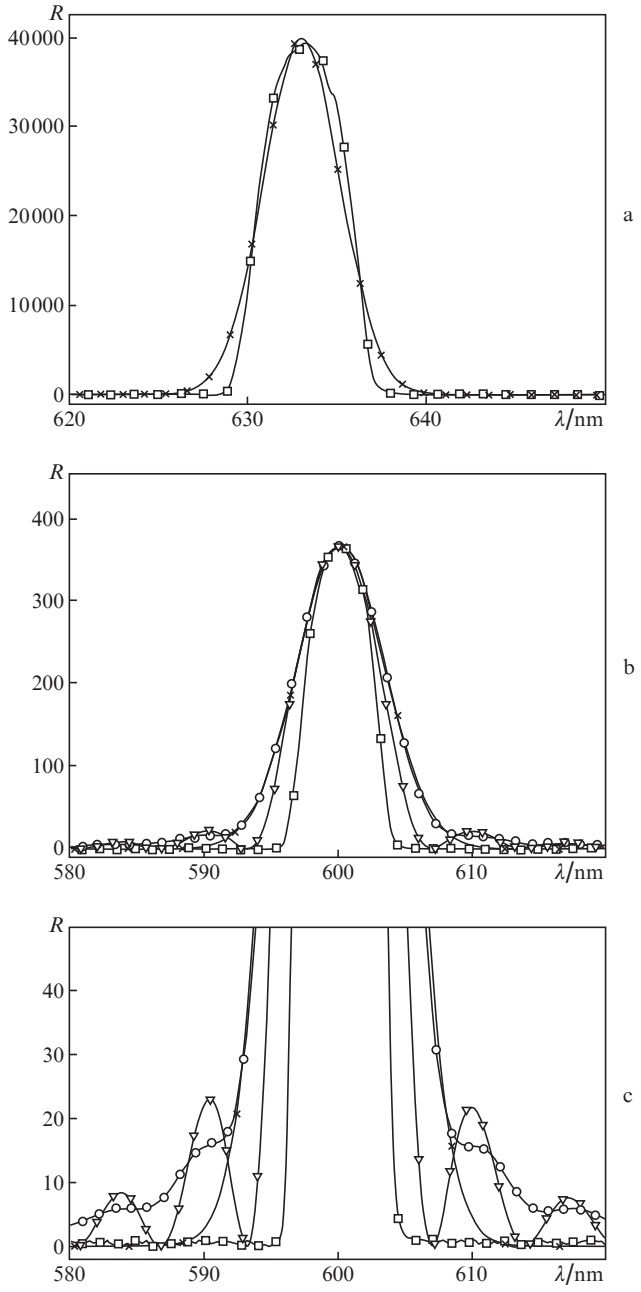

Figure 8. (a) Instrumental function of the spectrometer (□, spectral width 5.5 nm) and its approximation by a Gaussian function (×, width 5.0 nm), (b) the spectrum found using a computer model (▽, $H = 20$ μm, $\Delta n = 0.01$) and a convolution of the spectrum and instrumental function (○), and (c) the same as in panel b but on an enlarged scale.

Fig. 7). At large layer thicknesses, i.e., at smaller spectral widths, the lateral maxima become even less pronounced. For example, at $H = 60$ μm, they are transformed into a slowly decaying background. Undoubtedly, this is one of the main reasons for the absence of lateral maxima in the experimental spectra.

Another factor that may lead to the same effect is the decrease in the refractive index modulation depth near the holographic layer boundaries (i.e., apodization). For weak reflection (less than 10%), the spectral shape can in principle be found using integral (2) with a corresponding change in expression (3). However, this approach is invalid in the case of strong reflection. Figure 9 shows the changes in the spectrum with a change in the apodization function, which were calculated using our program for a 20-μm-thick layer. An isosceles trapezoid was applied as an apodization function: the amplitude of the variable part of the permittivity of free space in both transition regions changed linearly from zero at the layer boundary to the maximum value (0.005). Figure 9 shows the results for the transition-region sizes equal to zero (apodization is absent) and 1–10 μm (for a triangular apodization function). It can be seen that an increase in the transition region width leads to spectral broadening, reduction of the intensity in the maximum, and suppression of the lateral maxima. For a triangular function, the amplitude of the first lateral maximum decreases by more than two orders of magnitude.

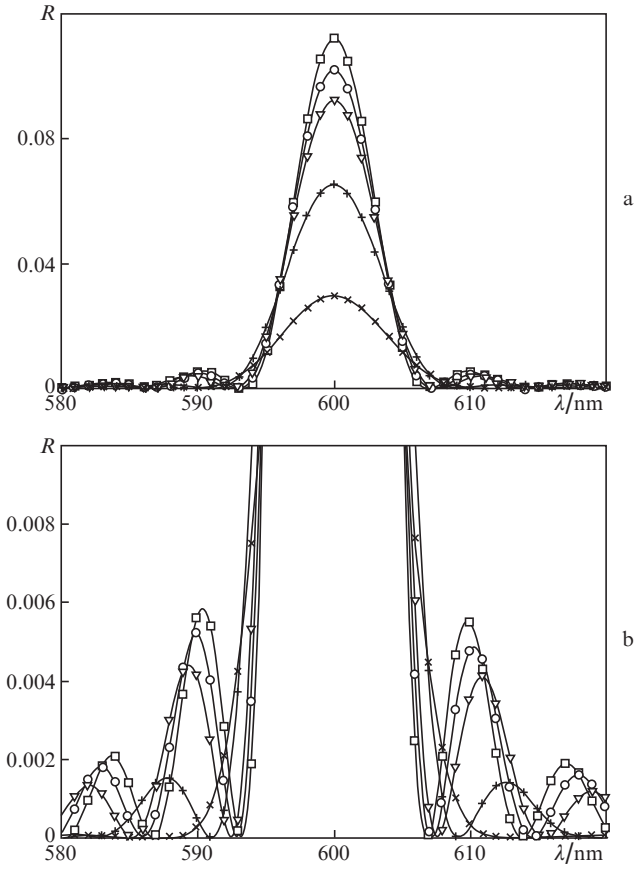

Figure 9. Reflection spectrum of a 20-μm-thick holographic layer (refractive index modulation depth 0.01), found using a computer model of apodization of the variable part of the refractive index at a zero width of the transition region (□) and for widths of (◇) 1, (▽) 2, (+) 5, and (×) 10 μm.

Thus, the developed model makes it possible to solve the problem of wave propagation in a more complex medium. In practice, both above-described effects, related to the distortion of the reflection band shape, will yield underestimated values of thickness if the hologram parameters are determined disregarding the broadening factors. This effect is less considerable when the spectral width of reflected light significantly exceeds the instrumental function width. The broadening can be taken into account when processing the spectrum with the aid of deconvolution algorithms for the spectrometer instrumental function.

10. Thus, we have proposed an algorithm for determining the parameters of a holographic nonabsorbing layer (its thickness and the amplitude of the variable part of its refractive index) from the parameters of the Bragg dip in the transmission spectrum of this layer (the relative amplitude of the dip and its width). The results of applying this algorithm to some experimental spectra are presented.

A computer model has been used to analyse possible reasons for the deviation of the spectral shape of the observed Bragg reflection and the dip in the transmission spectrum from the function $\sin x/x$: finite width of the instrumental function and decrease in the amplitude of the variable part of the refractive index near the holographic layer boundaries.

The differences in the reflection spectra of a layer in a periodic medium, obtained by the coupled-wave analysis and direct calculation of the field propagation in this layer, are considered for weak reflection.

In the case of weak reflection, analytical expressions have been derived for the spectrum within the single-reflection approximation, and these expressions have been analysed with allowance for the generally rejected values, leading to a spectrum asymmetry with respect to the resonant wavelength.

Within the direct calculation, we have considered (using a computer model) the behaviour of the reflection spectra of a holographic layer in a wide range of its parameters and proposed (based on the changes in the spectral shape of the reflection band in the layer spectrum) some criteria for classifying the reflection regimes from the layer.

Acknowledgements. This study was supported by a grant within the Fundamental Research Program 'Fundamental Sciences for Medicine' of the Presidium of the Russian Academy of Sciences.

References

1. Marshall A.J., Lowe Ch.R., et al. *J. Phys. Condens. Matter*., **18**, 619 (2006); Lowe Ch.R., Millington R.B., Bluth J., Mayes J.E. US Patent № 5989923 from 23.11.1999.
2. Kraiskii A.V., Postnikov V.A., Sultanov T.T., Khamidulin A.V. *Kvantovaya Elektron*., **40** (2), 178 (2010) [*Quantum Electron*., **40** (2), 178 (2010)].
3. Brillouin L., Parodi M. *Propagation des ondes dans les milieux periodiques* (Light Propagation in Periodic Structures) (Paris: Masson et Cie, 1956; Moscow: Inostr. Lit., 1959).
4. Born M., Wolf E. *Principles of Optics: Electromagnetic Theory of Propagation, Interference, and Diffraction of Light* (Oxford: Pergamon, 1964; Moscow: Nauka, 1979).
5. Kogelnik H. *Bell Syst. Techn. J*., **48**, 2909 (1969).
6. Yariv A., Yeh P. *Optical Waves in Crystals: Propagation and Control of Laser Radiation* (New York: Wiley, 1984; Moscow: Mir, 1987).
7. Colier R., Burckhardt C., Lin L. *Optical Holography* (New York: Academic, 1971; Moscow: Mir, 1973).
8. Krupitskii E.I., Chernov B.K. *Mater. VI Vsesoyuznoi shkoly po golografii* (Proc. VI All-Union School on Holography) (Leningrad, 1974) p. 46.
9. Brotherton-Ratcliffe D. In: *Holography – Basic Principles and Contemporary Applications*. Ed. by Dr. E. Mihaylova (InTech, 2013). DOI: 10.5772/53413. Available from: http://www.intechopen.com/books/holography-basic-principles-and-contemporary-applications/ understanding-diffraction-in-volume-gratings-and-holograms.
10. Putilin E.S. *Opticheskie pokrytiya. Uchebnoe posobie* (Optical Coatings: A Handbook) (St. Petersburg: Izd-vo ITMO, 2010).
11. Kolachevskii N.N., Pirozhkov A.S., Ragozin E.N. *Kvantovaya Elektron*., **30** (5), 428 (2000) [*Quantum Electron*., **30** (5), 428 (2000)].
12. Postnikov V.A., Kraiskii A.V, Sergienko I. In: *Holography – Basic Principles and Contemporary Applications*. Ed. by Dr. E. Mihaylova (InTech, 2013). DOI: 10.5772/53564. Available from: http://www.intechopen.com/books/holography-basic-principles-and-contemporary-applications/holographic-sensors-for-detection-of-components-in-water-solutions.
13. Burenkov D.S., Uspenskii Yu.A., Artyukov I.A., Vinogradov A.V. *Kvantovaya Elektron*., **35** (2), 195 (2005) [*Quantum Electron*., **35** (2), 195 (2005)].
14. Vishnyakov E.A., Kamenets F.F., Kondratenko V.V., Luginin M.S., Panchenko A.V., Pershin Yu.P., Pirozhkov A.S., Ragozin E.N. *Kvantovaya Elektron*., **42** (2), 143 (2012) [*Quantum Electron*., **42** (2), 143 (2012)].